Al-Nahrain Journal for Engineering Sciences **NJES**27(1)54-60, 2024
http://doi.org/10.29194/NJES.27010054

Laser Produced Hydrophilic and Hydrophobic Silicon Surfaces

A. A. Hatem*[1a], B. G. Rasheed[1b], Naser M. Ahmed[2]

Authors affiliations:

1*) Department of Laser & Optoelectronics Engineering, College of Engineering, Al-Nahrain University, Baghdad, Iraq.
a) aarafalsarah@gmail.com
b)b.g.rasheed@nahrainuniv.edu.iq

2) University Sains, Penang, Malaysia.

Paper History:

Received:15th Dec. 2023

Revised: 29th Dec. 2023

Accepted: 9th Jan. 2024

Abstract

Two lasers were utilized for silicon processing using photoelectrochemical etching and laser texturing in order to produce nano/micro structures, respectively. Photoelectrochemical etching process utilizes a CW diode laser of 532 nm wavelength was used to support electrochemical etching for both n-type and p-type conductivity. While laser texturing process was employed using pulsed fiber laser of 1064 nm wavelength. Various characterization methods were devoted to examine silicon micro/nanostructures surfaces produced by lasers. These methods include AFM, SEM and Raman scattering to provide clear evidence about formation of micro/nanostructures abundant at silicon surfaces. Moreover, FTIR analysis for the laser produced silicon surfaces could emphasize whether the resultant silicon surface is hydrophilic or hydrophobic. Image analysis software adopted a side view micro image was used to measure the contact angle between the water droplet and silicon micro/nano-surfaces. It is found that the laser produced silicon nanostructure by photoelectrochemical etching creates a hydrophobic surface and even super hydrophobic with contact angle of 130 degrees for 50 nm average size. In addition, utilizing fiber laser of high repetition rate for laser texturing produces microstructures that are super hydrophilic with contact angle could reach 8 degrees for a surface dimension of 50 µm.

Keywords: Silicon Micro/Nanostructure, Hydrophobic, Hydrophilic.

أنتاج أسطح السيليكون المايكروية / النانوية بالليزر القابلة والطاردة للماء

اعراف عبد المنعم حاتم ، بسام غالب رشيد ، ناصر محمود احمد

الخلاصة:

تم استخدام نوعين من الليزر لمعالجة سطح السيليكون بطريقة النقش الكهروكيميائي الضوئي والتركيب بالليزر لإنتاج أسطح نانوية ومايكروية على التوالي.في عملية النقش الكهروكيميائي الضوئي تم استخدام ليزر الدايود الذي يعمل بالنمط المستمر وبطول موجي يبلغ ٥٣٢ نانومتر لدعم النقش الكهروكيميائي لكلا النوعين من السيليكون نوع n ونوع p. بينما في عملية تركيب السطح بالليزر تم استخدام الفايبر ليزر الذي يعمل بالنمط النبضي بطول موجي ١٠٦٤ نانومتر. تم استخدام طرق مختلفة لتشخيص سطح السيليكون النانوي والمايكروي الناتج بواسطة الليزر. هذه الطرق تتضمن AFM, SEM وRaman scattering لتقديم دليل واضح حول تكوين الهياكل المايكروية / النانوية المتواجدة على أسطح السيليكون. بالإضافة الى ذلك فان فحص FTIR للأسطح الناتجة بالليزر تبين فيما إذا كان السطح محب او طارد للماء. تم استخدام برنامج لتحليل الصور اعتمادا على صورة جانبية للقطرة وذلك لقياس زاوية الاتصال بين قطرة الماء واسطح السيليكون المايكروية والنانوية. لقد تبين ان السطح النانوي للسيليكون ذو حجم ٥٠ نانومتر المنتج بواسطة الليزر عن طريق النقش الكهروكيميائي الضوئي يكون طارد للماء بزاوية اتصال تبلغ ١٣٠°. بالإضافة الى ذلك فان السطح المايكروي المنتج باستخدام الفايبر ليزر بمعدل تكرار عالي بحجم ٥٠ مايكرومتر يكون محبا للماء بزاوية اتصال تصل الى ٨°.

1. Introduction

Micro and nanotechnology have advanced considerably over the course of the last two decades. The introduction of micro/Nano scale features has generated a diverse variety of possibilities for enhancing surface properties, hence exerting a substantial influence on surface characteristics. By altering the angle of contact between drops and a micro/nanostructure, the hierarchical micro/nanostructure enhances the hydrophilic or hydrophobic impact. Therefore, to increase

NJES is an **open access Journal** with **ISSN 2521-9154** and **eISSN 2521-9162**

hydrophobicity, it is important to create micro/nanostructured surfaces [1].

The surface structure can be modified by altering the surface chemistry, adding buildings to a present surface, or combining the aforementioned techniques in different ways, or all three. Micro/nanostructured surfaces can be created through a variety of techniques, including electrochemical deposition, chemical ablation, and laser surface treatments [2].

The interplay between laser and substance is a unique technique for preparation of micro/nanostructure surfaces. When a nanosecond laser beam is focused onto the surface of a substance, the laser's energy undergoes a conversion process into thermal energy, which is then absorbed by the substance [1]. The substance rapidly becomes hot and melts, creating a molten puddle. The melted substance is cooled and solidified once more when the laser is turned off to create the micro/nanostructure. As a result, the process of creating micro/nanostructure by laser is greatly influenced by the nature of the material[3]. Since the silicon band gap energy (1.12 eV) is exactly equivalent to the laser photon energy when 1064 nm wavelength was used, resonance absorption occurs and this helps to control features of the micro/nanostructured silicon layer [4].

A solid surface's hydrophilicity and hydrophobicity are significantly influenced by the geometry of each surface [5]. It is one among topics covered by surface chemistry studies, where it is crucial to understand how intermolecular interactions affect surface properties [5]. To achieve the required hydrophobic or hydrophilic surface, great effort is made to change the surface chemistry of diverse solid surfaces [6-8]. The creation of hydrophobic and hydrophilic surfaces on a range of materials is one of the study fields that is progressing quickly [9].

The leaves of various plants, including lotus leaves, rose petals, and animals like Namib desert beetles, have been widely reported to exhibit unique wetting properties, including water-repelling or super-hydrophobicity and readily rolling off the surface, super-wicking effect, or wettability patterns with hydrophilic and hydrophobic patches, which allow to successfully store the fog droplets [9].

Many numerous and potential applications of hydrophobic and hydrophilic surfaces like coatings that prevent ice [10,11], self-cleaning metal surfaces, bactericidal and moisture coatings for paper and textiles [12-14] and micro fluidics, electrochemistry and biological analysis [15-17] and many others. Hydrophobic surfaces have garnered significant interest due to their potential applications in micro fluids and functional surfaces, particularly in the automotive and aerospace sectors [18].

An often-seen phenomenon is the presence of a static contact angle of about 90 degrees between the surface and a water droplet. Contact angles greater than this angle exhibit a hydrophobic effect, and for higher than 150 degrees are utilized for super-hydrophobic surfaces. While when they are lower than 90 degrees, they will be suitable for hydrophilic surfaces [19].

Hydrophobic materials are well acknowledged as highly favored and effective materials for industrial applications owing to their many benefits, including the inherent ability of a material or surface to cleanse itself, having the ability to decrease drag, anti-biofouling characteristics, and the ability of a material to withstand the process of corrosion [20-21]. Moreover, surfaces can be utilized in anti-fogging applications where clear vision is crucial, like windshields or swimming goggles [22]. Furthermore, Anti-fouling surfaces are crucial in biological applications and maritime engineering because they can stop microorganisms from settling into a ship's bottom. The development of a fine layer of water-based barriers delays the adhesion of microorganisms, biomedical applications, filters, heat pipes, and several other items [23].

The objective of this study is to elucidate the methodologies used in generating hydrophobic Si surfaces by laser-based procedures, which are contingent upon the specific micro and nanostructural characteristics. This feature is significantly important in many applications such as solar cells.

2. The Experimental Work

A-Materials & Methods

Various methods were used to create micro/nanostructure surfaces on p-type and n-type crystalline silicon wafers of dimensions 50 mm x 50 mm and 500μm thickness. The objective of this work was to investigate the hydrophobic and hydrophilic properties of these surfaces after laser processing.

A Teflon cell has been constructed to produce a nanostructured layer on the silicon wafer's surface by phptoelectrochemical etching process. The present design has considered for selective etching process of a single side of the wafer by the immersion silicon wafer in hydrofluoric (HF) acid with concentration (40%) and subjected to the diode laser irradiation with a wavelength (532nm), power (100 mW) and irradiation time (20 min) by photoelectrochemical etching [4]. The range of etching current densities was in the range (of 5-20 mA/cm2), and the laser spot diameter was (2 mm), while the backside of the wafer was completely separated from the etching acid. The photon energy of the diode laser (2.33 eV) was almost twice of that for silicon's band gap energy (1.12 eV), therefore, this laser was suitable for photoelectrochemical etching due to photo-absorption.

B-The experimental setup

The experimental set up for the photoelectrochemical etching process is shown in figure 1a. This process produces a nanostructured surface on n-type and p-type silicon wafers. Moreover, the laser texturing is a method that use a fiber laser to generate microstructures on the surface of silicon wafers, as seen in Figure (1b), with wavelength (1064 nm), spot diameter (50 μm), and power (1-30 W).

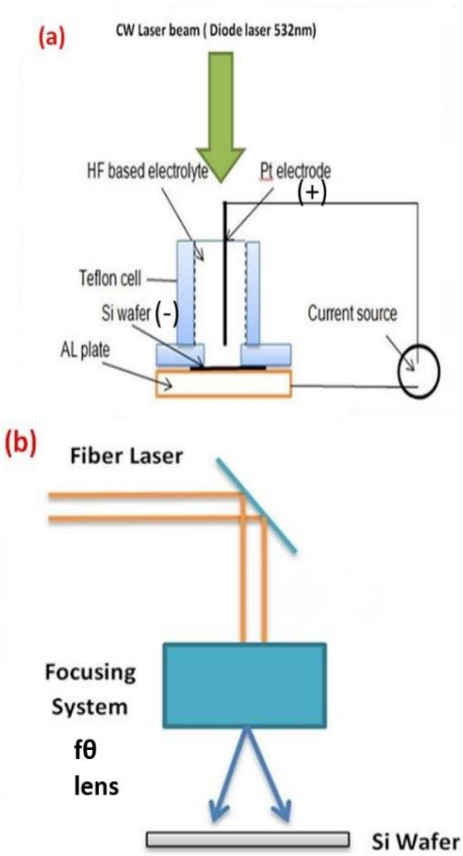

Figure (1): The experimental setup for (a) The PEC etching and (b) laser texturing by fiber laser.

High-resolution optical microscope supplied with a digital camera (OLYMPUS BX60M) was used to capture an image between the water droplet and micro/nano silicon surfaces. Then, optical image software (image j) was used to analyze and measure the contact angle.

Figure 2(a & b) reveal the formation of micro-structured silicon surfaces produced by photoelectrochemical and laser ablation techniques.

While SEM and AFM analysis were also employed to examine the nanostructured silicon surfaces. Moreover, Raman spectroscopy was used to ensure the formation of micro/nano silicon surfaces using (Ramanor 210). While, FTIR analysis was used to investigate the surface chemistry and hydrophobicity/hydrophilicity after laser processing.

Diffuse reflectance spectrum was also conducted for the three silicon samples bare, nanostructured surface prepared by photoelectrochemical etching and micro-structured surface prepared by laser texturing using (AvaLight-DH-S-BAL). This device has a deuterium halogen source of a very dominant alpha peak at 656 nm in which a dichroic filter was used to drastically reduce the interference effect. A comparison spectrum, which is taken with a standard AvaSpec-ULS2048CL. The light source delivers a continuous spectrum with high efficiency. The highest stability is in the ultraviolet, visible and near infrared range, from 200 to 1000 nm.

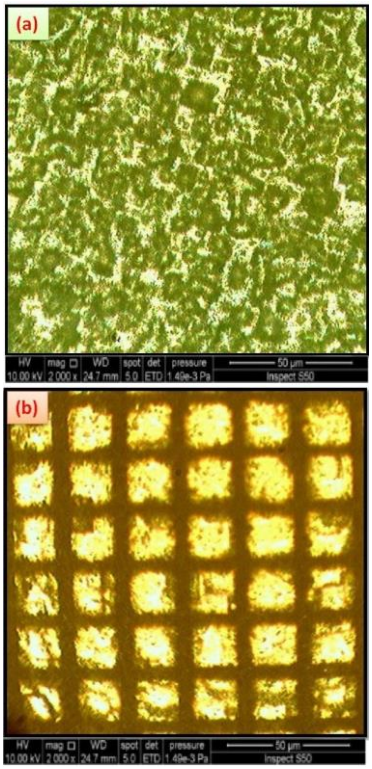

Figure (2): (a) The micro-structured surface (200X) on the silicon wafer produced by diode laser (Photoelectrochemical),(b) The microstructure (200X) created on the silicon surface produced by fiber laser (laser texturing).

3. Results and Discussions

A photoelectrochemical (PEC) etching process was employed to synthesize nanostructured silicon surfaces with various morphologies. Electrochemical dissolution in a hydrofluoric acid solution supported with optical radiation from a CW diode laser has created the porous layer with a depth of 30µm, as shown in Figure (3).

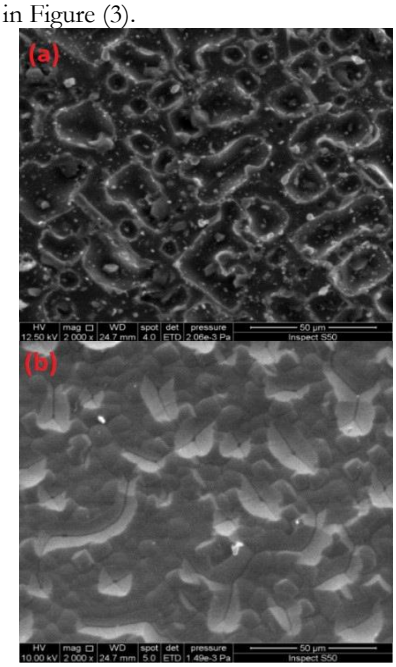

Figure (3): The SEM for micro/nanostructured: (a)Silicon n-type and (b)Silicon p-type.

The SEM micrographs in Figure (3) reveal the formation of a porous layer in n-type Silicon, as shown in Fig (3a). While column- like structure was observed for p-type Silicon, as shown in Fig (3b). This is attributed to the effect of extra holes supplied by the external source for p-type Silicon, which extremely facilitates the etching process when these holes form bonds with fluorine ions in the HF acid and subsequently detach silicon atoms from the surface. Moreover, the nanostructured layer at the silicon surface was investigated also by AFM. Figure (4) shows the nanostructured surface morphology for n-type and p-type silicon. The corresponding histogram for both substrates are shown in Figure (5). These histograms indicate the formation of a homogeneous Gaussian size distribution with average size of (150nm) and (90nm) for n-type and silicon p-type, respectively. This size distribution belongs to the Gaussian distribution of the laser intensity.

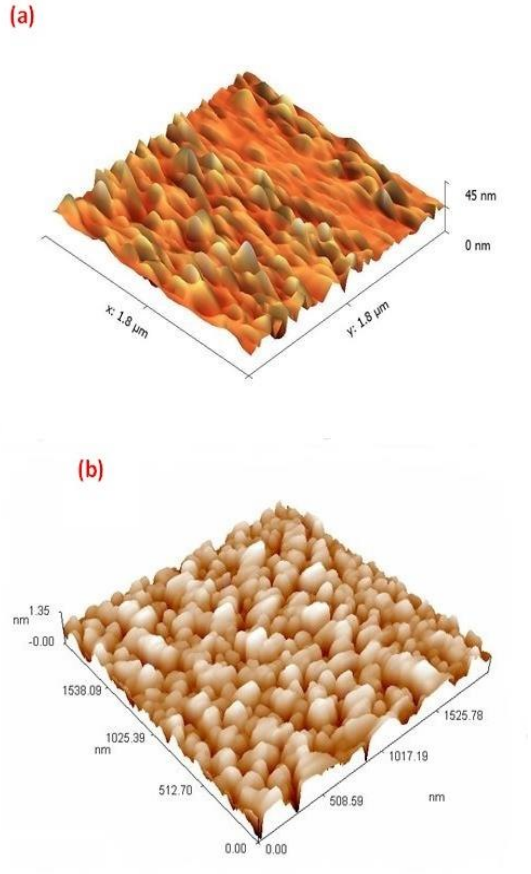

Figure (4) The AFM image for the nanostructure by PEC for: (a)Silicon n-type and (b)Silicon p-type wafers.

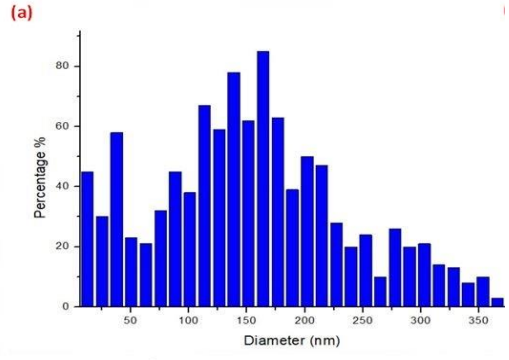

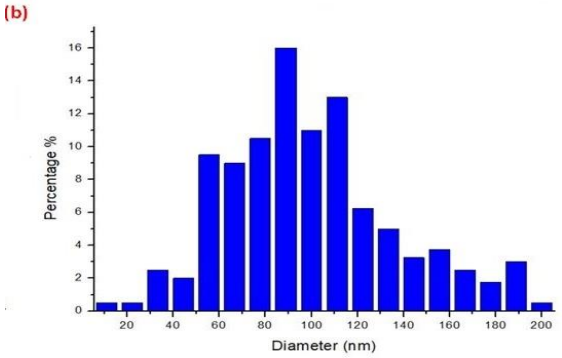

Figure (5): The histogram of the nanostructure for (a) n-type (b) p-type silicon wafer.

The hydrophobicity comparison between the non-treated silicon surface and laser treated surfaces is shown in figures 6 and 7. It is found that the contact angle (65°) for bare silicon surface. This contact angle becomes (130°) when the silicon surface is modified to etching process, as given in Table (1) and shown in Figure (6) and figure (7).

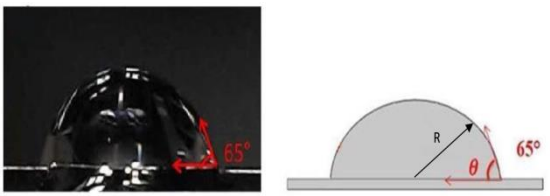

Figure (6): Water droplet upon the bare silicon surface.

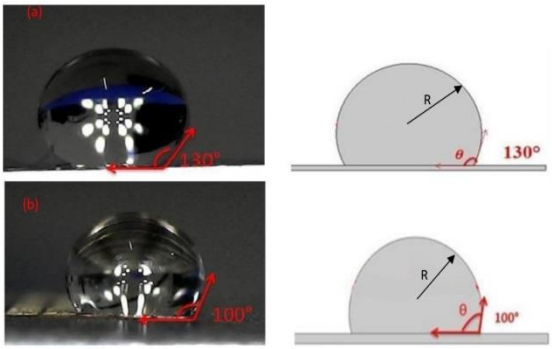

Figure (7): Water droplet upon the silicon surface produced by PEC for a: n-type and b: p-type.

Table (1): The contact angle for the bare surface and the nano-surface for n and p-type Silicon with different average sizes.

	Contact angle (°) Average size (nm)		Surface area ($\frac{m^2}{cm^3}$)
n-type Silicon	Bare	65	3.8mm²
	50	130	390
	100	115	388
	150	100	384
	200	85	290
p-type Silicon	Bare	65	3.8mm²
	50	100	350
	100	90	296
	150	80	264
	200	70	136

For the laser texturing, micro-structured surfaces are established on the silicon wafers with different line spaces (50μm-300μm). Table (2) presents the contact angle between a water droplet and the surfaces of both bare Si and micro-structured surfaces ablated by fiber laser, as well as the corresponding surface areas.

Table (2) indicates that greater contact angles are observed for smaller microstructures, and that is attributed to the effect of large surface area corresponding to those structures, which in turn is affected by a higher adsorption effect between the surface and the water droplet.

Table (2): The contact angle and surface area for the bare Si surface and the ablated Si surfaces.

Micro structure(μm)	Contact angle(°)	Surface area($\frac{m^2}{cm^3}$)
Bare	65	$3.8(mm)^2$
50	20	250
100	17	217
150	15	196
200	13	180
250	11	168
300	8	144

It is also found from Table (2) that the silicon wafer surface is converted to super hydrophilic, and a clear correlation was observed between the contact angle and the line spacing, as depicted in Figure (8). Incensing the surface line spacing (the microstructure dimension) leads to decrease the contact angle as well as the surface area and this is attributed to the reduced air gap which isolates the surface and the water droplet and subsequently, enhance the surface hydrophilicity.

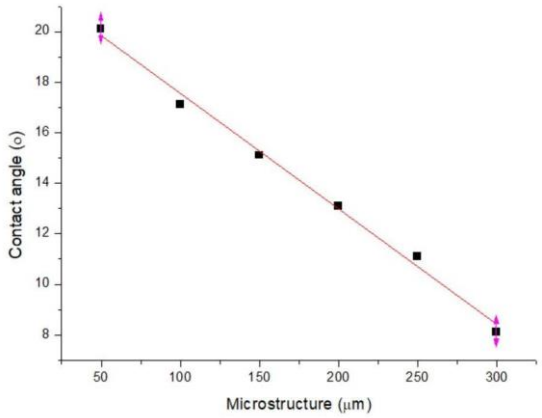

Figure (8): The relation between the hydrophobicity water droplet and Si surface by altering the line space.

Raman scattering is the inelastic scattering of light by material, which involves not only an energy transfer but a shift in the orientation of the light also. As input light from a visible laser is reduced to lower energies, a molecule normally gains excitation energy throughout this process.

Raman scattering was performed with the help of a dual monochromator (Jobin-Yvon), CW argon-ion laser, and electronics for counting photons are conducted in the back-scattering pattern for reconstructed silicon surfaces compared with polished (bare) silicon.

In contrast to the Raman natural line from Si crystalline, which has a sharp and symmetrical line shape of (10 cm-1) FWHM centered at (520 cm-1). While for silicon produced by photoelectrochemical, the Raman line becomes wider of (200 cm-1) FWHM and asymmetric, as depicted in Figure (9). It is also found that the Raman shift for the micro/nano surface produced by the electrochemical etching lies between the Raman natural line at (520 cm-1) and that for the structure produced by photoelectrochemical and has a FWHM of (110 cm-1). This indicates that larger size for nanostructure is established by electrochemical etching compared with that produced by photoelectrochemical etching [4].

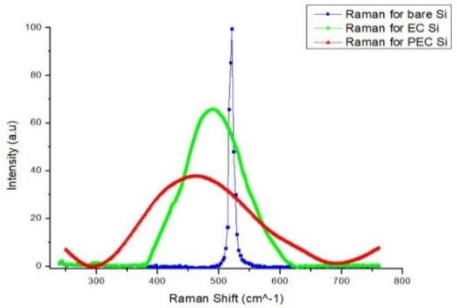

Figure (9): Raman shift for natural Silicon, nanostructure Si prepared by photoelectrochemical (PEC), and Si prepared by Electrochemical (EC).

Table (3) gives the Raman shift for the Silicon-wafer when etched with HF acid (EC) and exposed to the laser (PEC).

Table (3): Raman line shift for various silicon surfaces.

Material	Raman Shift (cm^{-1})	Average Size (nm)	Contact Angle (degree)	FWHM (cm)-1
Bare	____	____	65°	10
EC.	30	400μm	95°	110
PEC	90	180 nm	130°	200

The Fourier-transform infrared spectroscopy (FTIR) technique can be used to produce an IR spectrum of an object's emission or absorption [24]. Fourier Transform Infrared Spectroscopy (FTIR) finds widespread use across several disciplines such as organic synthesis, polymer research, petrochemical engineering, the pharmaceutical industry, and the inspection of food. The use of an FTIR spectrometer allows for the simultaneous acquisition of high-resolution spectral data across a broad range of wavelengths. FTIR spectrometers may be coupled with chromatography to enable the investigation of chemical reaction mechanisms and the identification of unstable compounds. Figure (10) illustrates the position of the emission or absorption and the peaks of these groups for the laser processed silicon.

It is found that a hydrophobic surface repels water and, as a result of its non-polar nature, is not miscible in water. Some of the most frequent chemical groups

found in hydrophobic compounds include -CH3, -CH2-CH3, -R-C6H5, and C2H2, whereas chemical species found in hydrophilic substances include -OH, -COO, and -NH. For silicon nanostructures prepared by photochemical etching, many peaks are observed in FTIR spectrum in figure (10a). One peak position on (1731 cm-1), corresponds to C-H bending, the class is an aromatic compound, and it is weak, or the group is C=O stretching, the class is a carboxylic acid, and it is strong. While the peak position at (1621 cm-1), is related to the group C=O stretching, the class is δ-lactam, and it is strong, or the group is C=C stretching and it is medium. Furthermore, the peak position at (1040 cm-1), is related to CO-O-CO stretching and the class is an anhydride which is strong and broad.

Moreover, FTIR spectrum of silicon microstructure produced by laser texturing with fiber laser surface has also examined, as shown in Figure (10 b), the peak position on (2917 cm-1) is related to the group O-H stretching, which is strong and broad. Therefore, this peak indicates the presence of O-H bond, which is refer to hydrophilic property, but it could also mean that it has an N-H bond, which is less hydrophilic.

Table (4): FTIR main peaks for silicon micro/nanostructures.

Material	FTIR Peak (cm-1)	Bond
Nanostructured Silicon	1731	C-H
	1621	C=O
	1040	CO-O-CO
Micro-structured silicon	2917	O-H

The surface reflectance could provide valuable details about the surface absorbance specialty when it is proposed to be used in solar cells. The surface reflectance of silicon nanostructures produced by photoelectrochemical etching and microstructures prepared by laser texturing compared with that of polished silicon were measured using diffuse reflectance set up. Figure (11) shows a remarkable decrease in the surface reflectance when the polished surface was converted to micro-structured and becomes very low at the visible region which has a high intensity for the sunlight spectrum. This can be explained due to the large surface area of the nanostructured surface. Therefore, nanostructured silicon surface is preferable for solar cell applications.

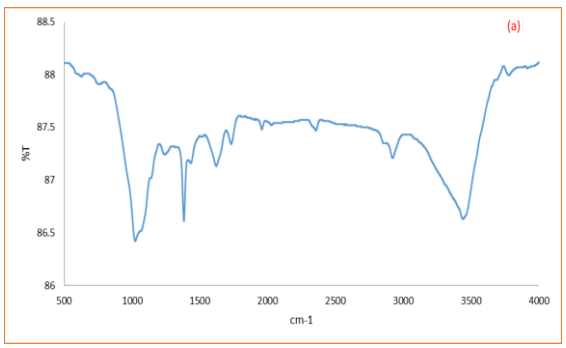

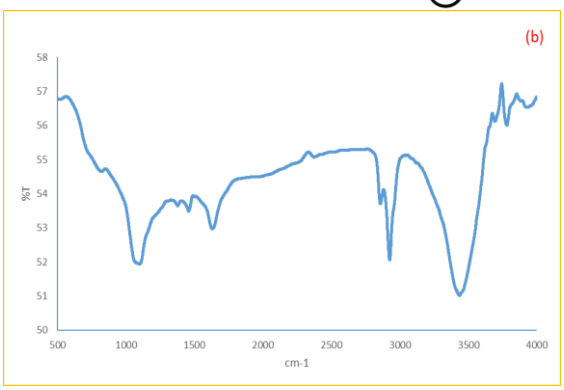

Figure (10): The FTIR spectrum of silicon surface produced by a) photoelectrochemical etching with diode laser and b) laser texturing with fiber laser.

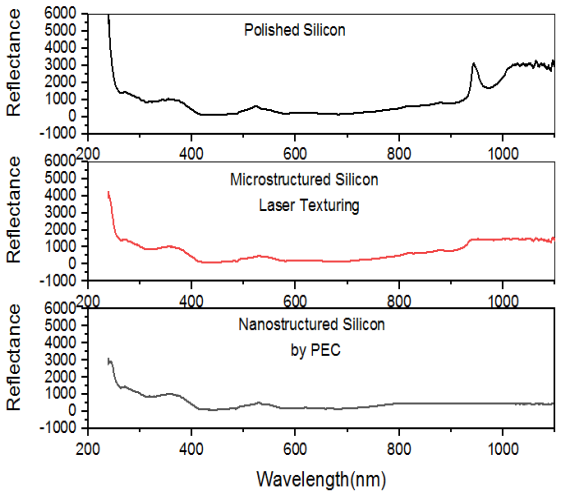

Figure (11): The reflectance spectrum for various silicon surfaces.

4. Conclusions

Laser micro/nano processing of silicon can be carried out by fiber laser texturing and also by photoelectrochemical etching using CW diode laser.

Silicon hydrophobic and hydrophilic surfaces can be effectively controlled by laser processing parameters.

Silicon nanostructures produced by photoelectrochemical etching with diode laser exhibit hydrophobic surfaces with contact angles greater than 90 degree. While microstructured silicon surfaces produced by fiber laser offer hydrophilic property and even superhydrophilicity with contact angle reach 8 degrees. The surface chemistry reveal formation of CH bonds for nanostructured silicon which indicates that the surface is hydrophobic, while O-H bonds was observed for microstructured silicon surface to form a hydrophilic surfaces.

5. Acknowledgments

We feel responsible to acknowledge Laser and Optoelectronics Engineering department, College of Engineering, Al-Nahrain University for their help and support.

6. References:

[1] T. Hang, A. Hu, H. Ling, M. Li, and D. Mao, "Super-hydrophobic nickel films with micro-nano

hierarchical structure prepared by electrodeposition," Applied Surface Science, vol. 256, no. 8, pp. 2400–2404, Feb. 2010.

[2] H. Zhang, J. Yang, B. Chen, C. Liu, M. Zhang, and C. Li, "Fabrication of superhydrophobic textured steel surface for anti-corrosion and tribological properties," Applied Surface Science, vol. 359, pp. 905–910, Dec. 2015.

[3] L. B. Boinovich, E. B. Modin, A. R. Sayfutdinova, K. A. Emelyanenko, A. L. Vasiliev, and A. M. Emelyanenko, "Combination of Functional Nanoengineering and Nanosecond Laser Texturing for Design of Superhydrophobic Aluminum Alloy with Exceptional Mechanical and Chemical Properties," ACS Nano, vol. 11, no. 10, pp. 10113–10123, Sep. 2017.

[4] B. G. Rasheed, "Synthesis of Silicon Nanostructures: Comparative Study," Advances in Materials, vol. 2, no. 1, p. 6, 2013.

[5] S. K. Sethi, R. Gogoi, A. Verma, and G. Manik, "How can the geometry of a rough surface affect its wettability? - A coarse-grained simulation analysis," Progress in Organic Coatings, vol. 172, p. 107062, Nov. 2022.

[6] J. Liu et al., "Hydrophobic/icephobic coatings based on thermal sprayed metallic layers with subsequent surface functionalization," Surface & Coatings Technology, vol. 357, pp. 267–272, Jan. 2019.

[7] M. Flemming, L. Coriand, and A. Duparré, "Ultra-hydrophobicity Through Stochastic Surface Roughness," Journal of Adhesion Science and Technology, vol. 23, no. 3, pp. 381–400, Jan. 2009.

[8] R. S. Kurusu and N. R. Demarquette, "Surface modification to control the water wettability of electrospun mats," International Materials Reviews, vol. 64, no. 5, pp. 249–287, Jun. 2018.

[9] M. Srinivasarao, "Biomimetics: Bioinspired Hierarchical-Structured Surfaces for Green Science and TechnologyBiomimetics: Bioinspired Hierarchical-Structured Surfaces for Green Science and Technology, Bharat Bhushan, Springer, 2016 (2nd ed.)," Physics Today, vol. 70, no. 9, pp. 60–61, Sep. 2017.

[10] F. Wang, C. Li, Y. Lv, F. Lv, and Y. Du, "Ice accretion on superhydrophobic aluminum surfaces under low-temperature conditions," Cold Regions Science and Technology, vol. 62, no. 1, pp. 29–33, Jun. 2010.

[11] C. Antonini, M. Innocenti, T. Horn, M. Marengo, and A. Amirfazli, "Understanding the effect of superhydrophobic coatings on energy reduction in anti-icing systems," Cold Regions Science and Technology, vol. 67, no. 1, pp. 58–67, Jun. 2011.

[12] C.-H. Xue, S.-T. Jia, J. Zhang, and L.-Q. Tian, "Superhydrophobic surfaces on cotton textiles by complex coating of silica nanoparticles and hydrophobization," Thin Solid Films, vol. 517, no. 16, pp. 4593–4598, Jun. 2009.

[13] Z. Hu, X. Zen, J. Gong, and Y. Deng, "Water resistance improvement of paper by superhydrophobic modification with microsized CaCO3 and fatty acid coating," Colloids and Surfaces A: Physicochemical and Engineering Aspects, vol. 351, no. 1–3, pp. 65–70, Nov. 2009.

[14] M. Zhang, S. Wang, C. Wang, and J. Li, "A facile method to fabricate superhydrophobic cotton fabrics," Applied Surface Science, vol. 261, pp. 561–566, Nov. 2012.

[15] Q. Huang, L. Lin, Y. Yang, R. Hu, E. A. Vogler, and C. Lin, "Role of trapped air in the formation of cell-and-protein micropatterns on superhydrophobic/superhydrophilicmicrotemplated surfaces," Biomaterials, vol. 33, no. 33, pp. 8213–8220, Nov. 2012.

[16] J. Nie, Y. Zhang, H. Wang, S. Wang, and G. Shen, "Superhydrophobic surface-based magnetic electrochemical immunoassay for detection of Schistosoma japonicum antibodies," Biosensors and Bioelectronics, vol. 33, no. 1, pp. 23–28, Mar. 2012.

[17] C. Steffes, T. Baier, and S. Hardt, "Enabling the enhancement of electroosmotic flow over superhydrophobic surfaces by induced charges," Colloids and Surfaces A: Physicochemical and Engineering Aspects, vol. 376, no. 1–3, pp. 85–88, Feb. 2011.

[18] P. Zhang and F. Y. Lv, "A review of the recent advances in superhydrophobic surfaces and the emerging energy-related applications," Energy, vol. 82, pp. 1068–1087, Mar. 2015.

[19] J. Tam, G. Palumbo, and U. Erb, "Recent Advances in Superhydrophobic Electrodeposits," Materials, vol. 9, no. 3, p. 151, Mar. 2016.

[20] Su, Wenbo, et al. "Robust, Superhydrophobic Aluminum Fins with Excellent Mechanical Durability and Self-Cleaning Ability." Micromachines, vol. 14, no. 3, 1 Mar. 2023, p. 704.

[21] Fakhri, Mohammadali, et al. "Facile, Scalable, and Low-Cost Superhydrophobic Coating for Frictional Drag Reduction with Anti-Corrosion Property." Tribology International, vol. 178, Feb. 2023, p. 108091.

[22] Wahab, Izzati Fatimah, et al. "Fundamentals of Antifogging Strategies, Coating Techniques and Properties of Inorganic Materials; a Comprehensive Review." Journal of Materials Research and Technology, vol. 23, 1 Mar. 2023, pp. 687–714.

[23] J. A. Howarter and J. P. Youngblood, "Self-Cleaning and Next Generation Anti-Fog Surfaces and Coatings," Macromolecular Rapid Communications, vol. 29, no. 6, pp. 455–466, Mar. 2008.

[24] D. R. Smith, R. L. Morgan, and E. V. Loewenstein, "Comparison of the Radiance of Far-Infrared Sources," Journal of the Optical Society of America, vol. 58, no. 3, p. 433, Mar. 1968.